

# A First Exposure to Statistical Mechanics for Life Scientists: Applications to Binding

Hernan G. Garcia<sup>1</sup>, Jané Kondev<sup>2</sup>, Nigel Orme<sup>3</sup>, Julie A. Theriot<sup>4</sup>, Rob Phillips<sup>5</sup>

<sup>1</sup>Department of Physics, California Institute of Technology, Pasadena, CA 91125, USA

<sup>2</sup>Department of Physics, Brandeis University Waltham, MA 02454, USA

<sup>3</sup>Garland Science Publishing, 270 Madison Avenue, New York, NY 10016, USA

<sup>4</sup>Department of Biochemistry, Stanford University School of Medicine, Stanford, CA 94305, USA

<sup>5</sup>Department of Applied Physics, California Institute of Technology, Pasadena, CA 91125, USA

September 17, 2007

## **Abstract**

Statistical mechanics is one of the most powerful and elegant tools in the quantitative sciences. One key virtue of statistical mechanics is that it is designed to examine large systems with many interacting degrees of freedom, providing a clue that it might have some bearing on the analysis of the molecules of living matter. As a result of data on biological systems becoming increasingly quantitative, there is a concomitant demand that the models set forth to describe biological systems be themselves quantitative. We describe how statistical mechanics is part of the quantitative toolkit that is needed to respond to such data. The power of statistical mechanics is not limited to traditional physical and chemical problems and there are a host of interesting ways in which these ideas can be applied in biology. This article reports on our efforts to teach statistical mechanics to life science students with special reference to binding problems in biology and provides a framework for others interested in bringing these tools to a nontraditional audience in the life sciences.

# 1 Does Statistical Mechanics Matter in Biology?

The use of the ideas of equilibrium thermodynamics and statistical mechanics to study biological systems are nearly as old as these disciplines themselves. Whether thinking about the binding constants of transcription factors for their target DNA or proteins on HIV virions for their target cell receptors, often the first discussion of a given problem involves a hidden assumption of equilibrium. There are two key imperatives for students of the life sciences who wish to explore the quantitative underpinnings of their discipline: i) to have a sense of when the equilibrium perspective is a reasonable approximation and ii) given those cases when it is reasonable, to know how to use the key tools of the calculus of equilibrium. Our experiences in teaching both undergraduate and graduate students in the life sciences as well as in participating both as students and instructors in the Physiology Course at the Marine Biological Laboratory in Woods Hole drive home the need for a useful introduction to statistical mechanics for life scientists.

This paper is a reflection of our attempts to find a minimalistic way of introducing statistical mechanics in the biological setting that starts attacking biological problems that students might care about as early as possible. We view this as part of a growing list of examples where quantitative approaches are included in the life sciences curriculum [1, 2, 3, 4, 5, 6]. As will be seen throughout the paper, one of the key components of this approach is to develop cartoons that provide a linkage between familiar biological concepts and their mathematical incarnation. The courses we teach often involve a very diverse mixture of students interested in how quantitative approaches from physics might be useful for thinking about living matter. On the one hand, we have biology students that want to make the investment to learn tools from physics. At the same time, about one third of our students are from that ever-growing category of physics students who are excited about taking what they know and using it to study living organisms. As a result, we face a constant struggle to not lose either the interest or understanding of one of these two constituencies. The challenge is to be interdisciplinary while maintaining strong contact with the core disciplines themselves.

One of the key questions that must be addressed at the outset has to do with the question of when equilibrium ideas are a viable approach in thinking about real biological problems.

Indeed, given the fact that biological systems are in a constant state of flux, it is reasonable to wonder whether equilibrium ideas are ever applicable. Nevertheless, there are a surprisingly large number of instances when the time scales conspire to make the equilibrium approach a reasonable starting point, even for examining some processes in living cells. To that end, we argue that the legitimacy of the equilibrium approach often centers on the question of *relative* time scales. To be concrete, consider several reactions linked together in a chain such as



For simplicity, we consider a set of reactions in which the terminal reaction is nearly irreversible. The thrust of our argument is that even though the conversion of  $B$  to  $C$  is bleeding off material from the  $A$  and  $B$  reaction, if the rate of  $B$  to  $C$  conversion is sufficiently slow compared to the back reaction  $B \rightarrow A$ , then the  $A \underset{k_-}{\overset{k_+}{\rightleftharpoons}} B$  reaction will always behave instantaneously as though it is in equilibrium. There are a range of similar examples that illustrate the way in which important biological problems, when boxed off appropriately, can be treated from the equilibrium perspective [7]. The goal of this paper is to use simple model problems to illustrate how equilibrium ideas can be exploited to examine biologically interesting case studies.

## 2 Boltzmann, Gibbs and the Calculus of Equilibrium

We find that statistical mechanics can be introduced in a streamlined fashion by proceeding axiomatically. We start by introducing a few key definitions and then arguing that just as classical mechanics can be built exclusively around repeated uses of  $\mathbf{F} = m\mathbf{a}$ , statistical mechanics has its own fundamental law (the Boltzmann distribution) from which results flow almost effortlessly and seemingly endlessly. There is a great deal of precedent for this axiomatic approach as evidenced by several amusing comments from well known statistical mechanics texts. In the preface to his book [8], Daniel Mattis comments on his thinking about what classes to take on statistical mechanics upon his arrival at graduate school. “I asked my classmate JR Schrieffer, who presciently had enrolled in that class, whether I should chance it later with a different instructor. He said not to bother - that he could explain all I needed to know about this topic over lunch. On a paper napkin, Bob wrote

$e^{-\beta H}$  “That’s it in a nutshell”. “Surely you must be kidding Mr. Schrieffer” I replied (or words to that effect) “How could you get the Fermi-Dirac distribution out of THAT?” “Easy as pie” was the reply ... and I was hooked”.

Similarly, in speaking of the Boltzmann distribution, Feynman notes in the opening volley of his statistical mechanics book: “This fundamental law is the summit of statistical mechanics, and the entire subject is either the slide-down from this summit, as the principle is applied to various cases, or the climb-up to where the fundamental law is derived...” [9]. Our sense is that in a first exposure to statistical mechanics for students of the life sciences, an emphasis on the slide-down from the summit which illustrates the intriguing applications of statistical mechanics is of much greater use than paining through the climb to that summit with a consideration of the nuances associated with where these distributions come from. As a result, we relegate a conventional derivation of the Boltzmann distribution to the appendix at the end of this paper.

So what is this “summit” that Feynman speaks of? Complex, many-particle systems such as the template DNA, nucleotides, primers and enzymes that make up a polymerase chain reaction, familiar to every biology student, can exist in an astronomical number of different states. It is the job of statistical mechanics to assign probabilities to all of these different ways (the distinct “microstates”) of arranging the system. The summit that Feynman speaks of is the simple idea that each of these different arrangements has a probability proportional to  $e^{-\beta E_i}$ , where  $E_i$  is the energy of the microstate of interest which is labeled by the index  $i$ . To make this seem less abstract, we begin our analysis of statistical mechanics by describing the notion of a microstate in a way that will seem familiar to biologists.

One of our favorite examples for introducing the concept of a microstate is to consider a piece of DNA from the bacterial virus known as  $\lambda$ -phage. If one of these  $\approx 48,500$  base pair long DNA molecules is fluorescently labeled and observed through a microscope as it jiggles around in solution, we argue that the different conformations adopted by the molecule correspond to its different allowed microstates. Of course, for this idea to be more than just words, we have to invoke some mathematical way to represent these different microstates. As shown in fig. 1, it is possible to characterize the states of a polymer such as DNA either discretely (by providing the  $x, y, z$  coordinates of a set of discrete points on the polymer) or continuously (by providing the position of each point on the polymer,  $\mathbf{r}(s)$ , as a function of

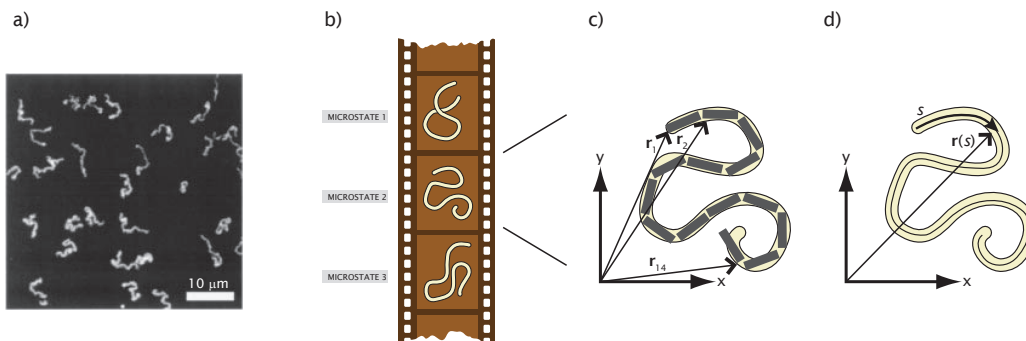


Figure 1: Microstates of DNA in solution. (a) Fluorescence microscopy images of  $\lambda$ -phage DNA [10] (reprinted with permission, copyright (1999) by the American Physical Society). The DNA molecule jiggles around in solution and every configuration corresponds to a different microstate. (b) The film strip shows how at every instant at which a picture is taken, the DNA configuration is different. From a mathematical perspective, we can represent the configuration of the molecule either by using (c) a discrete set of vectors  $\{\mathbf{r}_i\}$  or (d) by the continuous function  $\mathbf{r}(s)$ .

the distance  $s$  along the polymer).

A second way in which the notion of a microstate can be introduced that is biologically familiar is by discussing ligand-receptor interactions (and binding interactions more generally). This topic is immensely important in biology as can be seen by appealing to problems such as antibody-antigen binding, ligand-gated ion channels and oxygen binding to hemoglobin, for example [11, 12]. Indeed, Paul Ehrlich made his views on the importance of ligand-receptor binding evident through the precept: “Corpora non agunt nisi ligata - A substance is not effective unless it is linked to another” [12]. Whether discussing signaling, gene regulation or metabolism, biological action is a concert of different binding reactions and we view an introduction to the biological uses of binding and how to think about such binding using statistical mechanics as a worthy investment for biology and physics students alike.

To treat cases like these, it is convenient to imagine an isolated system represented by a box of solution which contains a single receptor and  $L$  ligands. One of the pleasures of using this example is that it emphasizes the simplifications that physicists love [13]. In particular, as shown in fig. 2, we introduce a lattice model of the solution in which the box is divided up into  $\Omega$  sub-boxes. These sub-boxes have molecular dimensions and can be occupied by only one ligand molecule at a time. We also assume that the concentration of ligand is so low

that they do not interact. This assumption is perfectly reasonable for the concentrations seen in solution biochemistry experiments but is far from valid in the crowded interior of the cell where the mean spacing between proteins is less than 10 nm. The study of crowding in the cellular interior is only now coming to the fore and providing a host of interesting challenges for physical scientists [14].

For the lattice model considered here, the different microstates correspond to the different ways of arranging the  $L$  ligands amongst these  $\Omega$  elementary boxes. Although it is natural for biological scientists who are accustomed to considering continuous functions and concentrations to chafe against the discretization of a solution in a lattice model, it is fairly easy to justify this simplification. We may choose any number of boxes  $\Omega$ , of any size. At the limit of a large number of very small boxes, they may have molecular dimensions. In practice, the mathematical results are essentially the same for most choices where  $\Omega \gg L$ , that is, where the solution is dilute. Given  $L$  ligands and  $\Omega$  sites that they can be distributed on, the total number of microstates available to the system (when no ligands are bound to the receptor) is

$$\text{number of microstates} = \frac{\Omega!}{L!(\Omega - L)!}. \quad (2)$$

The way to see this result is to notice that for the first ligand, we have  $\Omega$  distinct possible places that we can put the ligand. For the second ligand, we have only  $\Omega - 1$  choices and so on. However, once we have placed those ligands, we can interchange them in  $L!$  different ways without changing the actual microstate. In fact, these issues of rearrangement (distinguishability vs. indistinguishability) are subtle, but unimportant for our purposes since they don't change the ultimate results for classical systems such as the biological problems addressed here. We leave it as an exercise for the reader to show that the results in this paper would remain unaltered if considering the ligands to be distinguishable.

During our participation in the MBL Physiology Course in the summer of 2006, our favorite presentation of this notion of microstate was introduced by a PhD biology student from Rockefeller University. During her presentation, she used a box from which she cut out a square in the bottom. She then taped a transparency onto the bottom of the box and drew a square grid precisely like the one shown in fig. 2 and then constructed a bunch of "molecules" that just fit into the squares. Finally, she put this box on an overhead projector

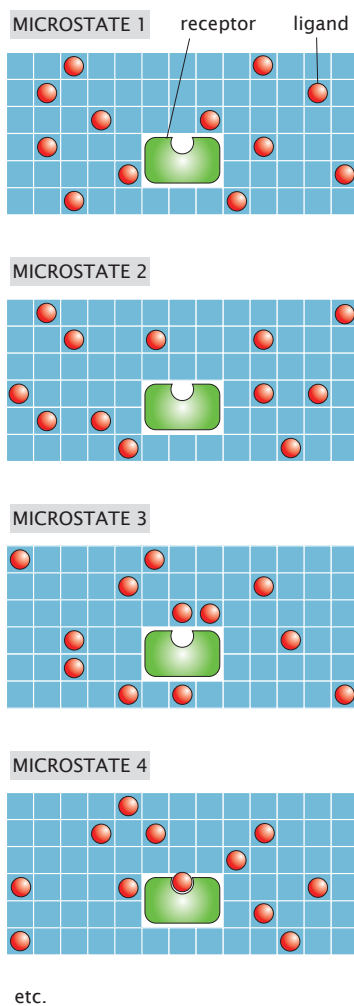


Figure 2: Lattice model for solution. Ligands in solution with their partner receptor. A simplified lattice model posits a discrete set of sites (represented as boxes) that the ligands can occupy and permits a direct evaluation of the various microstates (ways of arranging the ligands). The first three microstates shown here have the receptor unoccupied while the fourth microstate is one in which the receptor is occupied.

and shook it, repeatedly demonstrating the different microstates available to “ligands in solution”.

These different examples of microstates also permit us to give a cursory introduction to the statistical mechanical definition of entropy. In particular, we introduce entropy as a measure of microscopic degeneracy through the expression

$$S(V, N) = k_B \ln W(V, N), \quad (3)$$

where  $k_B = 1.38 \times 10^{-23}$  J/K the all-important constant of statistical mechanics known as the Boltzmann constant,  $S(V, N)$  is the entropy of an isolated system with volume  $V$  containing  $N$  particles, and  $W(V, N)$  is the number of distinct microstates available to that system. We also argue that the existence of the entropy function permits the introduction of the all-important variational statement of the second law of thermodynamics which tells us how to select out of all of the possible macrostates of a system, which state is most likely to be observed. In particular, for an isolated system (i.e. one that has rigid, adiabatic, impermeable walls, where no matter or energy can exit or enter the system) the equilibrium state is that macrostate that maximizes the entropy. Stated differently, the macroscopically observed state will be that state which can be realized in the largest number of microscopic states.

Now that we have the intuitive idea of microstates in hand *and* have shown how to enumerate them mathematically, and furthermore we have introduced Gibbs’ calculus of equilibrium in the form of the variational statement of the second law of thermodynamics, we are prepared to introduce the Boltzmann distribution itself. The Boltzmann distribution derives naturally from the second law of thermodynamics as the distribution that maximizes the entropy of a system in contact with a thermal bath (for a detailed derivation refer to the appendix). Statistical mechanics describes systems in terms of the probabilities of the various microstates. This style of reasoning is different from the familiar example offered by classical physics in disciplines such as mechanics and electricity and magnetism which centers on deterministic analysis of physical systems. By way of contrast, the way we do “physics” on systems that can exist in astronomical numbers of different microstates is to assign probabilities to them.

As noted above, one useful analogy is with the handling of classical dynamics. All science students have at one time or another been taught Newton’s second law of motion ( $\mathbf{F} = m\mathbf{a}$ ) and usually, this governing equation is introduced axiomatically. There is a corresponding central equation in statistical mechanics which can also be introduced axiomatically. In particular, if we label the  $i^{th}$  microstate by its energy  $E_i$ , then the probability of that microstate is given by

$$p_i = \frac{1}{Z} e^{-\beta E_i}, \quad (4)$$

where  $\beta = 1/k_B T$ . The factor  $e^{-\beta E_i}$  is called the Boltzmann Factor and  $Z$  is the “partition function”, which is defined as  $Z = \sum_i e^{-\beta E_i}$ . Note that from this definition it follows that the probabilities are normalized, namely  $\sum_i p_i = 1$ . Intuitively, what this distribution tells us is that when we have a system that can exchange energy with its environment, the probability of that system being in a particular microstate decays exponentially with the energy of the microstates. Further,  $k_B T$  sets the natural energy scale of physical biology where the temperature  $T$  for biological systems is usually around 300 K by telling us that microstates with energies too much larger than  $k_B T \approx 4.1 \text{ pN nm} \approx 0.6 \text{ kcal/mol} \approx 2.5 \text{ kJ/mol}$  are thermally inaccessible. This first introduction to the Boltzmann distribution suffices to now begin to analyze problems of biological relevance.

### 3 State Variables and States and Weights

One way to breathe life into the Boltzmann distribution is by constructing a compelling and honest correspondence between biological cartoons and their statistical mechanical meaning. Many of the cartoons familiar from molecular biology textbooks are extremely information-rich representations of a wealth of biological data and understanding. These informative cartoons can often be readily adapted to a statistical mechanics analysis simply by assigning statistical weights to the different configurations as shown in fig. 3. This first example considers the probability of finding an ion channel in the open or closed state in a simple model in which it is assumed that the channel can exist in only two states. We use ion channels as our first example of states and weights because, in this way, we can appeal to one of the physicists favorite models, the two-level system, while at the same time using a biological example that is of central importance. During our course, we try to repeat this

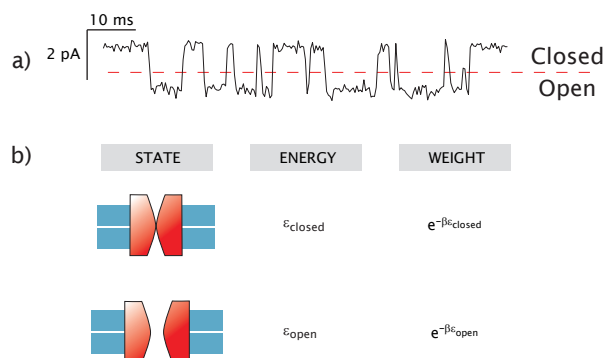


Figure 3: Ion channel open probability. (a) Current as a function of time for an ion channel showing repeated transitions between the open and closed states [15]. (b) States and weights for an ion channel. The cartoon shows a schematic of the channel states which have different energies, and by the Boltzmann distribution, different probabilities.

same basic motif of identifying in cartoon form the microscopic states of some biological problem and then to assign those different states and their corresponding statistical weights (and probabilities).

As shown in fig. 3, in the simplest model of an ion channel we argue that there are two states: the closed state and the open state. In reality some ion channels have been shown to exist in more than two states. However, the two state approximation is still useful for understanding most aspects of their electrical conductance behavior as shown by the trace in fig. 3a where only two states predominate. In order to make a mapping between the biological cartoon and the statistical weights, we need to know the energies of the closed and open states,  $\epsilon_{\text{closed}}$  and  $\epsilon_{\text{open}}$ . Also, for many kinds of channels the difference in energy between closed and open can be tuned by the application of external variables such as an electric field (voltage-gated channels), membrane tension (mechanosensitive channels) and the binding of ligands (ligand-gated channels) [16].

We find that a two-state ion channel is one of the cleanest and simplest examples for introducing how a statistical mechanics calculation might go. In addition, these ideas on ion channels serve as motivation for the introduction of a convenient way of characterizing the “state” of many macromolecules of biological interest. We define the two-state variables  $\sigma$  which can take on either the values 0 or 1 to signify the distinct conformation or state of binding of a given molecule. For example, in the ion channel problem  $\sigma = 0$  corresponds

to the closed state of the channel and  $\sigma = 1$  corresponds to the open state (this choice is arbitrary, we could equally have chosen to call  $\sigma = 1$  the closed state, but this choice makes more intuitive sense). As a result, we can write the energy of the ion channel as

$$E(\sigma) = (1 - \sigma)\epsilon_{\text{closed}} + \sigma\epsilon_{\text{open}}. \quad (5)$$

Thus, when the channel is closed,  $\sigma = 0$  and the energy is  $\epsilon_{\text{closed}}$ . Similarly, when  $\sigma = 1$ , the channel is open and the energy is  $\epsilon_{\text{open}}$ . Though this formalism may seem heavy handed, it is extremely convenient for generalizing to more complicated problems such as channels that can have a ligand bound or not as well being open or closed. Another useful feature of this simple notation is that it permits us to compute quantities of experimental interest straight away. Our aim is to compute the open probability  $P_{\text{open}}$  which, in terms of our state variable  $\sigma$ , can be written as  $\langle \sigma \rangle$ , where  $\langle \dots \rangle$  denotes an average. When  $\langle \sigma \rangle \approx 0$  this means that the probability of finding the channel open is low. Similarly, when  $\langle \sigma \rangle \approx 1$ , this means that it is almost certain that we will find the channel open. The simplest way to think of this average is to imagine a total of  $N$  channels and then to evaluate the fraction of the channels that are in the open state,  $N_{\text{open}}/N$ .

To compute the probability that the channel will be open, we invoke the Boltzmann distribution and, in particular, we evaluate the partition function given by

$$Z = \sum_{\sigma=0}^1 e^{-\beta E(\sigma)} = e^{-\beta\epsilon_{\text{closed}}} + e^{-\beta\epsilon_{\text{open}}}. \quad (6)$$

As noted above, for the simple two-state description of a channel, the partition function is a sum over only two states, the closed state and the open state. Given the partition function, we then know the probability of both the open and closed states via,  $p_{\text{open}} = e^{-\beta\epsilon_{\text{open}}}/Z$  and  $p_{\text{closed}} = e^{-\beta\epsilon_{\text{closed}}}/Z$ .

Using the partition function of eq. 6, we see that the open probability is given by (really, it is nothing more than  $p_{\text{open}}$ )

$$\langle \sigma \rangle = \sum \sigma p(\sigma) = 0 \times p(0) + 1 \times p(1). \quad (7)$$

As a result, we see that the open probability is given by

$$\langle \sigma \rangle = \frac{e^{-\beta \epsilon_{\text{open}}}}{e^{-\beta \epsilon_{\text{closed}}} + e^{-\beta \epsilon_{\text{open}}}} = \frac{1}{e^{\beta(\epsilon_{\text{open}} - \epsilon_{\text{closed}})} + 1}. \quad (8)$$

This result illustrates more quantitatively the argument made earlier that the energy scale  $k_B T$  is the standard that determines whether a given microstate is accessible. It also shows how in terms of energy what really matters is the relative difference between the different states ( $\Delta\epsilon = \epsilon_{\text{open}} - \epsilon_{\text{closed}}$ ) and not their absolute values. An example of the probability of the channel being open is shown in fig. 4 for several different choices of applied voltage in the case where the voltage is used to tune the difference between  $\epsilon_{\text{open}}$  and  $\epsilon_{\text{closed}}$ . In turn, measuring  $p_{\text{open}}$  experimentally tells you  $\Delta\epsilon$  between the two states.

Often, when using statistical mechanics to analyze problems of biological interest, our aim is to characterize several features of a macromolecule at once. For example, for an ion channel, the microstates are described by several “axes” simultaneously. Is there a bound ligand? Is the channel open or not? Similarly, when thinking about post-translational modifications of proteins, we are often interested in the state of phosphorylation of the protein of interest [18, 19]. But at the same time, we might wish to characterize the protein as being active or inactive, and also whether or not it is bound to allosteric activators or inhibitors. As with the ion channel, there are several variables needed to specify the overall state of the macromolecule of interest. Although this is admittedly oversimplified, countless biologically relevant problems can be approached by considering two main states (bound vs. unbound, active vs. inactive, phosphorylated vs. unphosphorylated, etc.) each of which can be characterized by its own state variable  $\sigma_i$ . The key outcome of this first case study is that we have seen how both the Boltzmann distribution and the partition function are calculated in a simple example and have shown a slick and very useful way of representing biochemical states using simple two-state variables.

## 4 Ligand-Receptor Binding as a Case Study

The next step upward in complexity is to consider ligand-receptor interactions where we must keep track of two or more separate molecules rather than just one molecule in two

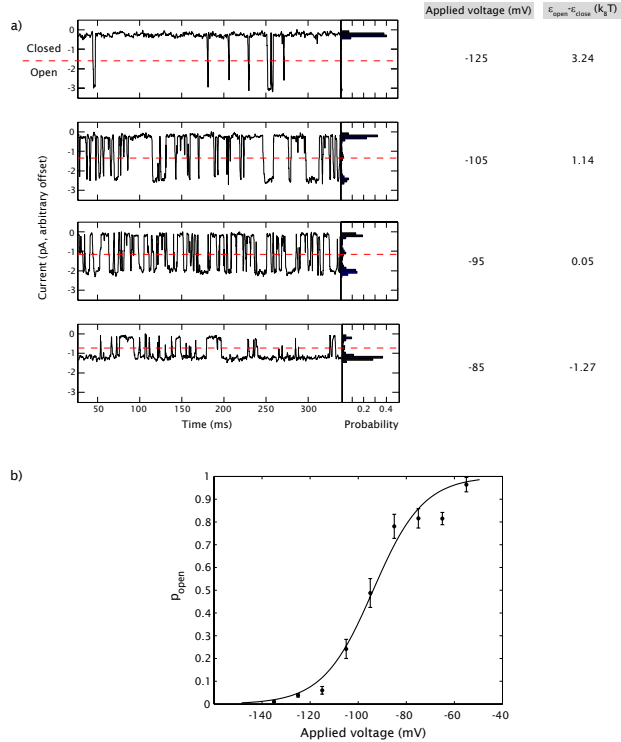


Figure 4: Probability of open and closed states for a voltage-sensitive ion channel. (a) Current traces for a sodium channel for four different applied voltages. The histograms to the right of each current trace show the fraction of time spent in the two states [17]. (b) Probability that the channel is open as a function of the applied voltage. The data points correspond to computing the fraction of time the channel spends open for traces like those shown in (a). The curve shows a fit to the data using eq. 8, where  $\beta(\epsilon_{\text{open}} - \epsilon_{\text{closed}}) = \beta\alpha(V_{\text{applied}} - V_0)$ . The fit yields  $\alpha \simeq -0.096 k_B T/\text{mV}$  and  $V_0 = -94 \text{ mV}$ .

different states. Examples of this kind of binding include: the binding of acetylcholine to the nicotinic acetylcholine receptor [20], the binding of transcription factors to DNA [21], the binding of oxygen to hemoglobin [22], the binding of antigens to antibodies [23] and so on. To examine the physics of fig. 2, imagine there are  $L$  ligand molecules in the box characterized by  $\Omega$  lattice sites as well as a single receptor with one binding site as shown. Our ambition is to compute the probability that the receptor will be occupied ( $p_{bound}$ ) as a function of the number (or concentration) of ligands.

To see the logic of this calculation more clearly, fig. 5 shows the states available to this system as well as their Boltzmann factors, multiplicities (i.e. the number of different ways of arranging  $L$  or  $L - 1$  ligands in solution) and overall statistical weights which are the products of the multiplicities and the Boltzmann factor. The key point is that there are only two classes of states: i) all of those states for which there is no ligand bound to the receptor and ii) all of those states for which one of the ligands is bound to the receptor. The useful feature of this situation is that although there are many realizations of each class of state, the Boltzmann factor for each of these individual realizations for each of the classes of state are all the same as shown in fig. 5 since all microstates in each class have the same energy.

To compute the probability that the receptor is occupied, we need to construct a ratio in which the numerator involves the accumulated statistical weight of all states in which one ligand is bound to the receptor and the denominator is the sum over all states. This idea is represented graphically in fig. 6. What the figure shows is that there are a host of different states in which the receptor is occupied: first, there are  $L$  different ligands that can bind to the receptor, second, the  $L - 1$  ligands that remain behind in solution can be distributed amongst the  $\Omega$  lattice sites in many different ways. In particular, we have

$$\text{weight when receptor occupied} = \underbrace{e^{-\beta\epsilon_{\text{bound}}}}_{\text{receptor}} \times \underbrace{\sum_{\text{solution}} e^{-\beta(L-1)\epsilon_{\text{solution}}}}_{\text{free ligands}}, \quad (9)$$

where we have introduced  $\epsilon_{\text{bound}}$  as the energy for the ligand when bound to the receptor and  $\epsilon_{\text{solution}}$  as the energy for a ligand in solution. The summation  $\sum_{\text{solution}}$  is an instruction to sum over all of the ways of arranging the  $L - 1$  ligands on the  $\Omega$  lattice sites in solution

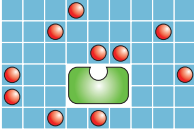
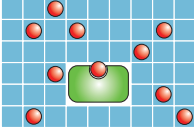
STATE	ENERGY	MULTIPLICITY	WEIGHT (MULTIPLICITY $\times$ BOLTZMANN WEIGHT)
	$L\epsilon_{\text{solution}}$	$\frac{\Omega!}{L!(\Omega-L)!} \approx \frac{\Omega^L}{L!}$	$\frac{\Omega^L}{L!} e^{-\beta L\epsilon_{\text{solution}}}$
	$(L-1)\epsilon_{\text{solution}} + \epsilon_{\text{bound}}$	$\frac{\Omega!}{(L-1)!(\Omega-L+1)!} \approx \frac{\Omega^{L-1}}{(L-1)!}$	$\frac{\Omega^{L-1}}{(L-1)!} e^{-\beta[(L-1)\epsilon_{\text{solution}} + \epsilon_{\text{bound}}]}$

Figure 5: States and weights diagram for ligand-receptor binding. The cartoons show a lattice model of solution for the case in which there are  $L$  ligands and  $\Omega$  lattice sites. In the upper panel, the receptor is unoccupied. In the lower panel, the receptor is occupied by a ligand and the remaining  $L - 1$  ligands are free in solution. A given state has a weight dictated by its Boltzmann factor. The multiplicity refers to the number of different microstates that share that same Boltzmann factor (for example, all of the states with no ligand bound to the receptor have the same Boltzmann factor). The total statistical weight is given by the product of the multiplicity and the Boltzmann factor.

with each of those states assigned the weight  $e^{-\beta(L-1)\epsilon_{\text{solution}}}$ . Since the Boltzmann factor is the same for each of these states, what this sum amounts to is finding the number of arrangements of the  $L - 1$  ligands amongst the  $\Omega$  lattice sites and yields

$$\sum_{\text{solution}} e^{-\beta(L-1)\epsilon_{\text{solution}}} = e^{-\beta(L-1)\epsilon_{\text{solution}}} \frac{\Omega!}{(L-1)!(\Omega - (L-1))!}. \quad (10)$$

To effect this sum, we have exploited precisely the same counting argument that led to eq. 2 with the only change that now we have  $L - 1$  ligands rather than  $L$ . The denominator of the expression shown in fig. 6 is the partition function itself since it represents a sum over *all* possible arrangements of the system (both those with the receptor occupied and not) and is given by

$$Z(L, \Omega) = \underbrace{\sum_{\text{solution}} e^{-\beta L\epsilon_{\text{solution}}}}_{\text{none bound}} + e^{-\beta\epsilon_{\text{bound}}} \underbrace{\sum_{\text{solution}} e^{-\beta(L-1)\epsilon_{\text{solution}}}}_{\text{ligand bound}}. \quad (11)$$

We already evaluated the second term in the sum culminating in eq. 10. To complete our evaluation of the partition function, we have to evaluate the sum  $\sum_{\text{solution}} e^{-\beta L\epsilon_{\text{solution}}}$  over

$$p_{\text{bound}} = \frac{\sum_{\text{states}} \left( \text{Diagram 1} \right)}{\sum_{\text{states}} \left( \text{Diagram 2} \right) + \sum_{\text{states}} \left( \text{Diagram 3} \right)}$$

Figure 6: Probability of receptor occupancy. The figure shows how the probability of receptor occupancy can be written as a ratio of the weights of the favorable outcomes and the weights of *all* outcomes. In this case the numerator is the result of summing over the weights of all states in which the receptor is occupied.

all of the ways of arranging the  $L$  ligands on the  $\Omega$  lattice sites with the result

$$\sum_{\text{solution}} e^{-\beta L \epsilon_{\text{solution}}} = e^{-\beta L \epsilon_{\text{solution}}} \frac{\Omega!}{L!(\Omega - L)!}. \quad (12)$$

In light of these results, the partition function can be written as

$$Z(L, \Omega) = e^{-\beta L \epsilon_{\text{solution}}} \left[ \frac{\Omega!}{L!(\Omega - L)!} \right] + e^{-\beta \epsilon_{\text{bound}}} e^{-\beta(L-1)\epsilon_{\text{solution}}} \left[ \frac{\Omega!}{(L-1)!(\Omega - (L-1))!} \right]. \quad (13)$$

We can now simplify this result by using the approximation that

$$\frac{\Omega!}{(\Omega - L)!} \approx \Omega^L, \quad (14)$$

which is justified as long as  $\Omega \gg L$ . To see why this is a good approximation consider the case when  $\Omega = 10^6$  and  $L = 10$  resulting in

$$\frac{10^6!}{(10^6 - 10)!} = 10^6 \cdot (10^6 - 1) \cdot (10^6 - 2) \cdot \dots \cdot (10^6 - 9) \simeq (10^6)^{10}. \quad (15)$$

Note that the approximate result is the largest term in the sum which we obtain by multiplying out all the terms in parentheses. We leave it to the reader to show that the correction is of the order 0.001 %, five orders of magnitude smaller than the leading term.

With these results in hand, we can now write  $p_{\text{bound}}$  as

$$p_{\text{bound}} = \frac{e^{-\beta\epsilon_{\text{bound}}} \frac{\Omega^{L-1}}{(L-1)!} e^{-\beta(L-1)\epsilon_{\text{solution}}}}{\frac{\Omega^L}{L!} e^{-\beta L\epsilon_{\text{solution}}} + e^{-\beta\epsilon_{\text{bound}}} \frac{\Omega^{L-1}}{(L-1)!} e^{-\beta(L-1)\epsilon_{\text{solution}}}}. \quad (16)$$

This result can be simplified by multiplying the top and bottom by  $\frac{L!}{\Omega^L} e^{\beta L\epsilon_{\text{solution}}}$ , resulting in

$$p_{\text{bound}} = \frac{e^{-\beta\epsilon_{\text{bound}}} \frac{\Omega^{L-1}}{(L-1)!} e^{-\beta(L-1)\epsilon_{\text{solution}}}}{\frac{\Omega^L}{L!} e^{-\beta L\epsilon_{\text{solution}}} + e^{-\beta\epsilon_{\text{bound}}} \frac{\Omega^{L-1}}{(L-1)!} e^{-\beta(L-1)\epsilon_{\text{solution}}}} \times \frac{\frac{L!}{\Omega^L} e^{\beta L\epsilon_{\text{solution}}}}{\frac{L!}{\Omega^L} e^{\beta L\epsilon_{\text{solution}}}}. \quad (17)$$

We combine the two fractions in the previous equation and note that  $L!/(L-1)! = L$  and that  $e^{-\beta\epsilon_{\text{bound}}} e^{-\beta(L-1)\epsilon_{\text{solution}}} \times e^{-\beta L\epsilon_{\text{solution}}} = e^{-\beta(\epsilon_{\text{bound}} - \epsilon_{\text{solution}})}$ . Finally, we define the difference in energy between a bound ligand and a ligand that is free in solution as  $\Delta\epsilon = \epsilon_{\text{bound}} - \epsilon_{\text{solution}}$ . The probability of binding to the receptor becomes

$$p_{\text{bound}} = \frac{\frac{L}{\Omega} e^{-\beta\Delta\epsilon}}{1 + \frac{L}{\Omega} e^{-\beta\Delta\epsilon}}. \quad (18)$$

The overall volume of the box is  $V_{\text{box}}$  and this permits us to rewrite our results using concentration variables. In particular, this can be written in terms of ligand concentration  $c = L/V_{\text{box}}$  if we introduce  $c_0 = \Omega/V_{\text{box}}$ , a ‘‘reference’’ concentration where every lattice position in the solution is occupied. The choice of reference concentration is arbitrary. For the purposes of fig. 7 we choose the elementary box size to be  $1 \text{ nm}^3$ , resulting in  $c_0 \approx 0.6 \text{ M}$ . This is comparable to the standard state used in many biochemistry textbooks of  $1 \text{ M}$ . The binding curve can be rewritten as

$$p_{\text{bound}} = \frac{\frac{c}{c_0} e^{-\beta\Delta\epsilon}}{1 + \frac{c}{c_0} e^{-\beta\Delta\epsilon}}. \quad (19)$$

This classic result goes under many different names depending upon the field. In biochemistry, this might be referred to as a Hill function with Hill coefficient one. Chemists and physicists might be more familiar with this result as the Langmuir adsorption isotherm which provides a measure of the surface coverage as a function of the partial pressure or the concentration. Regardless of names, this expression will be our point of departure for thinking about all binding problems and an example of this kind of binding curve is shown in fig. 7. This reasoning can be applied to binding in real macromolecules of biological

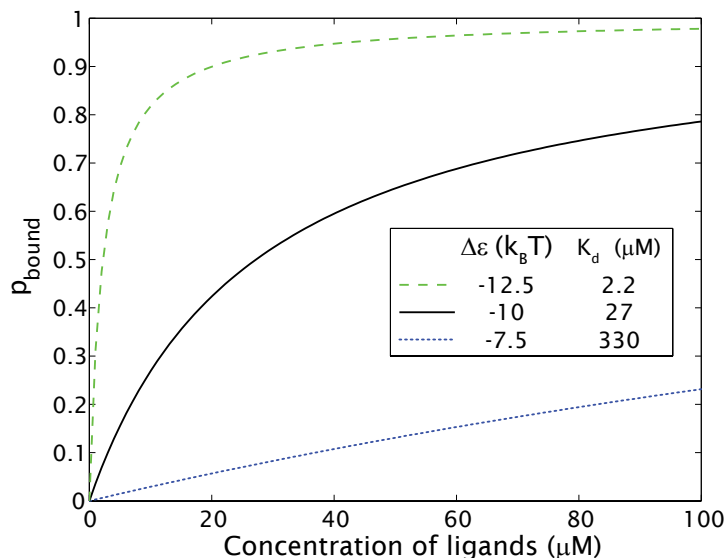


Figure 7: Simple binding curve. This curve shows  $p_{\text{bound}}$  as calculated in eq. 19. The different curves correspond to different choices for the strength of the ligand-receptor binding energy,  $\Delta\epsilon$ , given a reference concentration of  $c_0 = 0.6$  M. The corresponding dissociation constants are shown as well.

interest such as myoglobin and HIV viral proteins interacting with cell surface receptors as shown in fig. 8. Though many problems of biological interest exhibit binding curves that are “sharper” (i.e. there is a more rapid change in  $p_{\text{bound}}$  with ligand concentration) than this one, ultimately, even those curves are measured against the standard result derived here.

So far, we have examined binding from the perspective of statistical mechanics. That same problem can be addressed from the point of view of equilibrium constants and the law of mass action, and it is enlightening to examine the relation between the two points of view. To see the connection, the reaction of interest is characterized by the stoichiometric equation



This reaction is described by a dissociation constant given by the law of mass action as

$$K_d = \frac{[L][R]}{[LR]}. \quad (21)$$

It is convenient to rearrange this expression in terms of the concentration of ligand-receptor

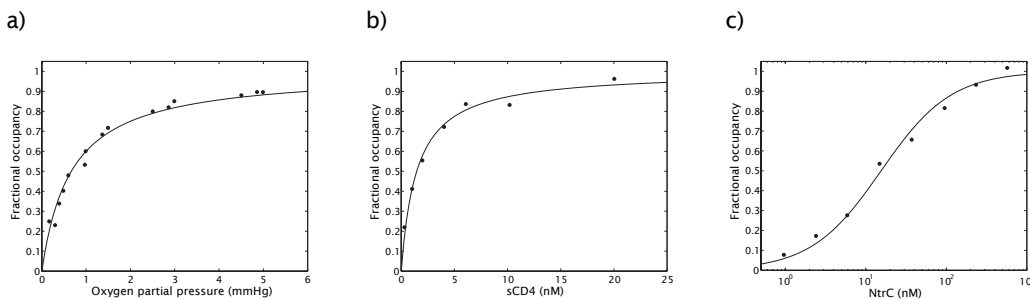


Figure 8: Examples of ligand-receptor binding. (a) The binding of oxygen to myoglobin as a function of the oxygen partial pressure. The points correspond to the measured occupancy of myoglobin as a function of the oxygen partial pressure [24] (because oxygen is a gas, partial pressure is used rather than concentration) and the curve is a fit based upon the one-parameter model from eq. 19. The fit yields  $\Delta\epsilon \approx -7.04 k_B T$  using a standard state  $c_0 = 760 \text{ mmHg} = 1 \text{ atm}$ , which also corresponds to a dissociation constant  $K_d = 0.666 \text{ mmHg}$ . (b) Binding of HIV protein gp120 to cell surface receptor sCD4 [25]. The standard state in this case is  $c_0 = 0.6M$  resulting in a binding energy of  $\Delta\epsilon \approx -19.84 k_B T$  and a dissociation constant of  $K_d = 1.4578 \text{ nM}$ . (c) Binding of NtrC to DNA [26]. The standard state in this case is  $c_0 = 0.6 M$  resulting in a binding energy of  $\Delta\epsilon = -17.47 k_B T$  and a dissociation constant  $K_d = 15.5 \text{ nM}$ .

complexes as

$$[LR] = \frac{[L][R]}{K_d}. \quad (22)$$

As before, our interest is in the probability that the receptor will be occupied by a ligand. In terms of the concentration of free receptors and ligand-receptor complexes,  $p_{\text{bound}}$  can be written as

$$p_{\text{bound}} = \frac{[LR]}{[R] + [LR]}. \quad (23)$$

We are now poised to write  $p_{\text{bound}}$  itself by invoking eq. 22, with the result that

$$p_{\text{bound}} = \frac{\frac{[L][R]}{K_d}}{[R] + \frac{[L][R]}{K_d}} = \frac{\frac{[L]}{K_d}}{1 + \frac{[L]}{K_d}}. \quad (24)$$

What we see is that  $K_d$  is naturally interpreted as that concentration of ligand at which the receptor has a probability of 1/2 of being occupied.

We can relate our two descriptions of binding as embodied in eqns. 19 and 24. Indeed, these two equations permit us to go back and forth between the statistical mechanical and thermodynamic treatment of binding through the recognition that the dissociation constant

can be written as  $K_d = c_0 e^{\beta\Delta\epsilon}$ . To see that, we note that both of these equations have the same functional form ( $p_{bound} = x/(1+x)$ ) allowing us to set  $[L]/K_d = \frac{c}{c_0} e^{-\beta\Delta\epsilon}$  and noting that  $[L] = c$  by definition. This equation permits us to use measured equilibrium constants to determine microscopic parameters such as the binding energy as illustrated in figs. 7 and 8.

## 5 Statistical Mechanics and Transcriptional Regulation

Transcriptional regulation is at the heart of much of biology. With increasing regularity, the data that is being generated on transcriptional regulation is quantitative. In particular, it is possible to quantify how much a given gene is expressed, where within the organism and at what time. Of course, with the advent of such data, it is important that models of transcriptional regulation keep pace with the measurements themselves. The first step in the transcription process is the binding of RNA polymerase to its target DNA sequence at the start of a gene known as a promoter. From a statistical mechanics perspective, the so-called “thermodynamic models” of gene expression are founded upon the assumption that the binding probability of RNA polymerase can be used as a surrogate for the extent of gene expression itself [27, 28, 21, 29]. Here too, the use of equilibrium ideas must be justified as a result of separation of time scales such that the binding step can equilibrate before the process of transcription itself begins. The formulations derived above can be directly applied to the process of transcription by binding of RNA polymerase to DNA. The fact that DNA is an extended, linear polymer makes it seem at first blush like a very different type of binding problem than the protein-ligand interactions discussed above. Nevertheless, as we will show below, these same basic ideas are a natural starting point for the analysis of gene expression.

The way we set up the problem is shown in fig. 9. First, we argue that the genome can be idealized as a “reservoir” of  $N_{NS}$  nonspecific binding sites. We assume that RNA polymerase may bind with its footprint starting at any base pair in the entire genome, and that almost all of these possible binding sites are nonspecific ones. For the case of *E. coli*, there are roughly 500 – 2,000 polymerase molecules for a genome of around  $5 \times 10^6$  base pairs [30]. Amongst these nonspecific sites, there is one particular site (the promoter for the

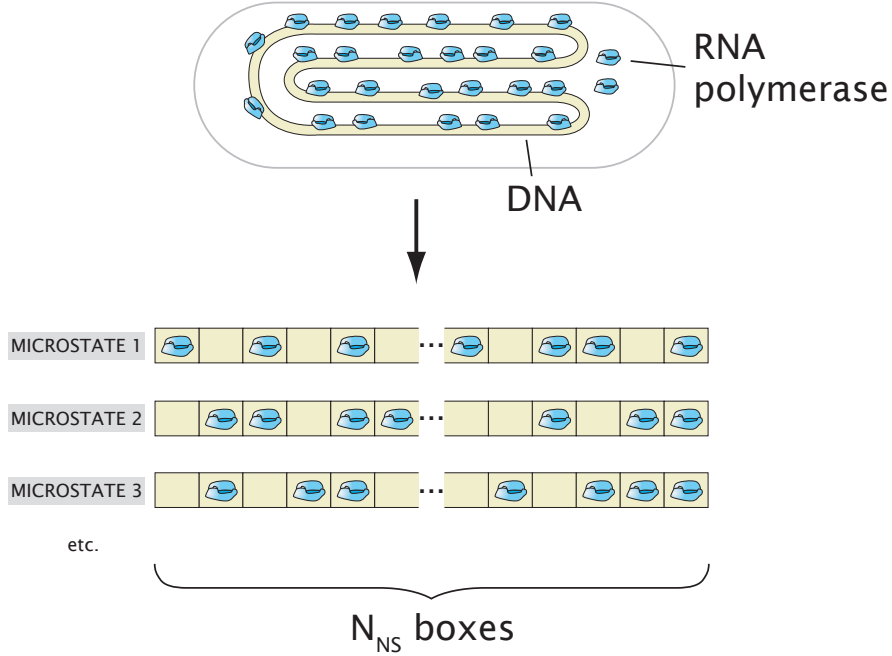


Figure 9: RNA polymerase nonspecific reservoir. This figure represents DNA as a series of binding sites (schematized as boxes) for RNA polymerase. The number of nonspecific binding sites is  $N_{NS}$ .

gene of interest) that we are interested in considering. In particular, we want to know the probability that this specific site will be occupied.

As noted above, the simplest model for RNA polymerase binding argues that the DNA can be viewed as  $N_{NS}$  distinct boxes where we need to place  $P$  RNA polymerase molecules, only allowing one such molecule per site. This results in the partial partition function characterizing the distribution of polymerase molecules on the nonspecific DNA as

$$Z_{NS}(P, N_{NS}) = \underbrace{\frac{N_{NS}!}{P!(N_{NS} - P)!}}_{\text{number of arrangements}} \times \underbrace{e^{-\beta P \epsilon_{pd}^{NS}}}_{\text{Boltzmann weight}}. \quad (25)$$

We will use the notation  $\epsilon_{pd}^S$  to characterize the binding energy of RNA polymerase to specific sites (promoters) and  $\epsilon_{pd}^{NS}$  to characterize the binding energy for nonspecific sites. (A note of caution is that this model is overly simplistic since there is a continuum of

different binding energies for the nonspecific sites [31].) We are now poised to write down the *total* partition function for this problem which broadly involves two classes of states: i) all  $P$  RNA polymerase molecules are bound nonspecifically (note the similarity to the partition function for ligand-receptor binding as shown in eq. 11), ii) one of the polymerase molecules is bound to the promoter and the remaining  $P - 1$  polymerase molecules are bound nonspecifically. Given these two classes of states, we can write the *total* partition function as

$$Z(P, N_{NS}) = \underbrace{Z_{NS}(P, N_{NS})}_{\text{empty promoter}} + \underbrace{Z_{NS}(P - 1, N_{NS})e^{-\beta\epsilon_{pd}^S}}_{\text{RNAP on promoter}}. \quad (26)$$

To find the probability that RNA polymerase is bound to the promoter of interest, we compute the ratio of the weights of the configurations for which the RNA polymerase is bound to its promoter to the weights associated with all configurations. This is presented schematically in fig. 10 and results in

$$p_{bound} = \frac{\frac{N_{NS}!}{(P-1)!(N_{NS}-P)!} e^{-\beta(P-1)\epsilon_{pd}^{NS}} e^{-\beta\epsilon_{pd}^S}}{\frac{N_{NS}!}{P!(N_{NS}-P)!} e^{-\beta P\epsilon_{pd}^{NS}} + \frac{N_{NS}!}{(P-1)!(N_{NS}-P)!} e^{-\beta(P-1)\epsilon_{pd}^{NS}} e^{-\beta\epsilon_{pd}^S}}. \quad (27)$$

Although this equation looks extremely grotesque it is really just the same as eq. 19 and is illustrated in fig. 10. In order to develop intuition for this result, we need to simplify the equation by invoking the approximation  $\frac{N_{NS}!}{(N_{NS}-P)!} \simeq (N_{NS})^P$ , which holds if  $P \ll N_{NS}$ . Note that this same approximation was invoked earlier in our treatment of ligand-receptor binding. In light of this approximation, if we multiply the top and bottom of eq. 27 by  $\left[ \frac{P!}{(N_{NS})^P} e^{\beta P\epsilon_{pd}^{NS}} \right]$ , we can write our final expression for  $p_{bound}$  as

$$p_{bound}(P, N_{NS}) = \frac{1}{\frac{N_{NS}}{P} e^{\beta(\epsilon_{pd}^S - \epsilon_{pd}^{NS})} + 1}. \quad (28)$$

Once again, it is the energy difference  $\Delta\epsilon$  that matters rather than the absolute value of any of the particular binding energies. Furthermore the difference between a strong promoter and a weak promoter can be considered as equivalent to a difference in  $\Delta\epsilon$  [21].

The problem of promoter occupancy becomes much more interesting when we acknowledge the fact that transcription factors and other proteins serve as molecular gatekeepers, letting RNA polymerase bind at the appropriate time and keeping it away from the pro-

$$p_{\text{bound}} = \frac{\sum_{\text{states}} \left( \text{Nonspecific DNA, Promoter, RNA polymerase} \right)}{\sum_{\text{states}} \left( \text{Nonspecific DNA, Promoter, RNA polymerase} \right) + \sum_{\text{states}} \left( \text{Nonspecific DNA, Promoter, RNA polymerase} \right)}$$

Figure 10: Probability of RNA polymerase binding. The probability of polymerase binding is constructed as a ratio of favorable outcomes (i.e. promoter occupied) to all possible outcomes. We are assuming that RNA polymerase is always bound to DNA, either specifically or nonspecifically.

motor at others. Different individual transcription factors can either activate the promoter through favorable molecular contacts between the polymerase and the activator or they can stand in the way of polymerase binding (this is the case of repressors). An example of repression is shown in fig. 11. The same ideas introduced above can be exploited for examining the competition between repressor and polymerase for two overlapping binding sites on the DNA. In this case, there are three classes of states to consider: i) empty promoter, ii) promoter occupied by RNA polymerase and iii) promoter occupied by repressor. In this case, the total partition function is given by

$$Z_{\text{tot}}(P, R, N_{NS}) = \underbrace{Z(P, R, N_{NS})}_{\text{empty promoter}} + \underbrace{Z(P-1, R, N_{NS})e^{-\beta\epsilon_{pd}^S}}_{\text{RNAP on promoter}} + \underbrace{Z(P, R-1, N_{NS})e^{-\beta\epsilon_{rd}^S}}_{\text{repressor on promoter}}, \quad (29)$$

where we have written the total partition function as a sum over partial partition functions which involve sums over certain restricted sets of states. Each  $Z$  is written as a function of  $P$  and  $R$ , the number of polymerases and repressors in the nonspecific reservoir, respectively. We have introduced  $\epsilon_{rd}$ , which accounts for the energy of binding of the repressor to a specific site ( $\epsilon_{rd}^S$ ) or to a nonspecific site ( $\epsilon_{rd}^{NS}$ ). For example, the term corresponding to the empty promoter can be written as

$$Z(P, R, N_{NS}) = \frac{N_{NS}!}{P!R!(N_{NS}-P-R)!} \times e^{-\beta P \epsilon_{pd}^{NS}} \times e^{-\beta R \epsilon_{rd}^{NS}}. \quad (30)$$

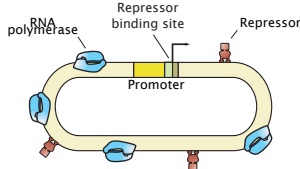
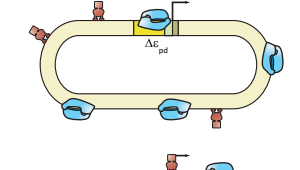
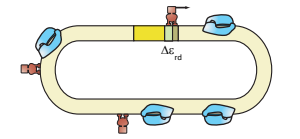
STATE	ENERGY	MULTIPLICITY	WEIGHT (MULTIPLICITY $\times$ BOLTZMANN WEIGHT)
	$R\epsilon_{rd}^{NS} + P\epsilon_{pd}^{NS}$	$\frac{N_{NS}!}{P! R! (N_{NS}-P-R)!} \approx \frac{(N_{NS})^{P+R}}{P! R!}$	$\frac{(N_{NS})^{P+R}}{P! R!} e^{-\beta R\epsilon_{rd}^{NS}} e^{-\beta P\epsilon_{pd}^{NS}}$
	$R\epsilon_{rd}^{NS} + (P-1)\epsilon_{pd}^{NS} + \epsilon_{pd}^S$	$\frac{N_{NS}!}{(P-1)! R! [N_{NS}-(P-1)-R]!} \approx \frac{(N_{NS})^{(P-1)+R}}{(P-1)! R!}$	$\frac{(N_{NS})^{(P-1)+R}}{(P-1)! R!} e^{-\beta R\epsilon_{rd}^{NS}} e^{-\beta(P-1)\epsilon_{pd}^{NS}} e^{-\beta\epsilon_{pd}^S}$
	$(R-1)\epsilon_{rd}^{NS} + P\epsilon_{pd}^{NS} + \epsilon_{rd}^S$	$\frac{N_{NS}!}{P! (R-1)! [N_{NS}-P-(R-1)]!} \approx \frac{(N_{NS})^{P+(R-1)}}{P! (R-1)!}$	$\frac{(N_{NS})^{P+(R-1)}}{P! (R-1)!} e^{-\beta(R-1)\epsilon_{rd}^{NS}} e^{-\beta P\epsilon_{pd}^{NS}} e^{-\beta\epsilon_{rd}^S}$

Figure 11: States and weights for promoter in the presence of repressor. The promoter is labeled in dark yellow and the repressor binding site (operator) is labeled in brown. Notice the overlap between the promoter and the repressor binding site, which is denoted in green. The weights of these different states are a product of the multiplicity of the state of interest and the corresponding Boltzmann factor.

The other two terms have the same form except that  $P$  goes to  $P - 1$  or that  $R$  goes to  $R - 1$ .

Once we have identified the various competing states and their weights, we are in a position to ask key questions of biological interest. For example, what is the probability of promoter occupancy as a function of repressor concentration? The results worked out above now provide us with the tools in order to evaluate the probability that the promoter will be occupied by RNA polymerase. This probability is given by the ratio of the favorable outcomes to all of the outcomes. In mathematical terms, that is

$$p_{bound}(P, R, N_{NS}) = \frac{Z(P-1, R, N_{NS})e^{-\beta\epsilon_{pd}^S}}{Z(P, R, N_{NS}) + Z(P-1, R, N_{NS})e^{-\beta\epsilon_{pd}^S} + Z(P, R-1, N_{NS})e^{-\beta\epsilon_{rd}^S}}. \quad (31)$$

As argued above, this result can be rewritten in compact form by dividing top and bottom

by  $Z(P-1, R, N_{NS})e^{-\beta\epsilon_{pd}^S}$  and by invoking the approximation

$$\frac{N_{NS}!}{P!R!(N_{NS}-P-R)!} \simeq \frac{(N_{NS})^P}{P!} \frac{(N_{NS})^R}{R!} \quad (32)$$

which amounts to the physical statement that there are so few polymerase and repressor molecules in comparison with the number of available sites,  $N_{NS}$ , that each of these molecules can more or less fully explore those  $N_{NS}$  sites without feeling the presence of each other. The resulting probability is

$$p_{\text{bound}}(P, R, N_{NS}) = \frac{1}{1 + \frac{N_{NS}}{P} e^{\beta(\epsilon_{pd}^S - \epsilon_{pd}^{NS})} \left(1 + \frac{R}{N_{NS}} e^{-\beta(\epsilon_{rd}^S - \epsilon_{rd}^{NS})}\right)}. \quad (33)$$

Of course, a calculation like this is most interesting when it sheds light on some experimental measurement. In this case, we can appeal to measurements on one of the classic regulatory networks in biology, namely, the *lac* operon. The *lac* promoter controls genes that are responsible for lactose utilization by bacteria. When the operon is “on”, the bacterium produces the enzymes necessary to import and digest lactose. By way of contrast, when the operon is “off”, these enzymes are lacking (or expressed at low “basal” levels). It has been possible to measure relative changes in the production of this enzyme as a function of both the number of repressor molecules and the strength of the repressor binding sites [32]. This relative change in gene expression is defined as the concentration of protein product in the presence of repressor divided by the concentration of protein product in the absence of it. In order to connect this type of data to the thermodynamic models we resort to one key assumption, namely that the level of gene expression is linearly related to  $p_{\text{bound}}$ , the probability of finding RNA polymerase bound to the promoter. Once this assumption is made, we can compute the fold-change in gene expression as

$$\text{fold-change in gene expression} = \frac{p_{\text{bound}}(R \neq 0)}{p_{\text{bound}}(R = 0)}. \quad (34)$$

After inserting eq. 33 in the expression for the fold-change we find

$$\text{fold-change in gene expression} = \frac{1 + \frac{N_{NS}}{P} e^{\beta(\epsilon_{pd}^S - \epsilon_{pd}^{NS})}}{1 + \frac{N_{NS}}{P} e^{\beta(\epsilon_{pd}^S - \epsilon_{pd}^{NS})} \left(1 + \frac{R}{N_{NS}} e^{-\beta(\epsilon_{rd}^S - \epsilon_{rd}^{NS})}\right)}. \quad (35)$$

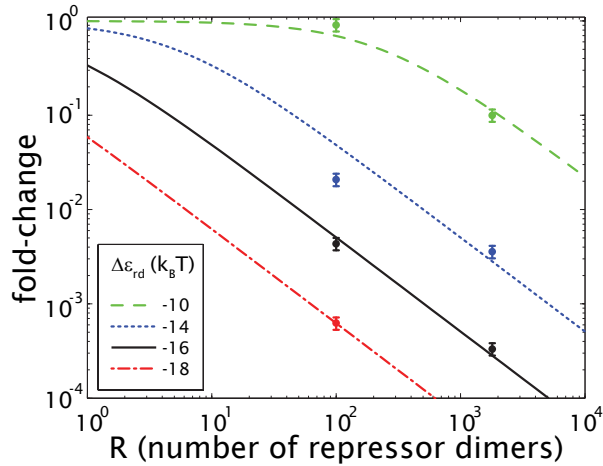


Figure 12: Fold-change due to repression. Experimental data on the fold-change in gene expression as a function of repressor concentration and binding affinity to DNA [32] and corresponding determination of the binding strength of repressor to DNA given by the theoretical model. Experimentally, the different binding strengths are changed by varying the DNA sequence of the site where repressor binds. For each one of these DNA constructs only one parameter, the difference in binding energy  $\Delta\epsilon$  is obtained using eq. 36.

Finally, we note that in the case of a weak promoter such as the *lac* promoter, *in vitro* measurements suggest that the factor  $\frac{N_{NS}}{P} e^{\beta(\epsilon_{pd}^S - \epsilon_{pd}^{NS})}$  is of the order of 500 [21]. This makes the second term in the numerator and denominator of eq. 35 much bigger than one. In this particular case of weak promoter the fold-change becomes independent of RNA polymerase as follows

$$\text{fold-change in gene expression} \simeq \frac{\frac{N_{NS}}{P} e^{\beta(\epsilon_{pd}^S - \epsilon_{pd}^{NS})}}{\frac{N_{NS}}{P} e^{\beta(\epsilon_{pd}^S - \epsilon_{pd}^{NS})} \left(1 + \frac{R}{N_{NS}} e^{-\beta(\epsilon_{rd}^S - \epsilon_{rd}^{NS})}\right)} = \left(1 + \frac{R}{N_{NS}} e^{-\beta(\epsilon_{rd}^S - \epsilon_{rd}^{NS})}\right)^{-1}. \quad (36)$$

For binding to a strong promoter, this approximation is no longer valid since the factor  $\frac{N_{NS}}{P} e^{\beta(\epsilon_{pd}^S - \epsilon_{pd}^{NS})}$  is of order 3 in this case. In fig. 12 we show the experimental data for different concentrations of repressor and values of its binding relative affinity to DNA,  $\Delta\epsilon_{rd} = \epsilon_{rd}^S - \epsilon_{rd}^{NS}$ . Overlaid with this data we plot the fold-change in gene expression given by eq. 36 where the binding strength to each type of site is determined. Notice that for each curve there is only one parameter to be determined,  $\Delta\epsilon_{rd}$ . This simple example shows how statistical mechanics arguments can be used to interpret measurements on gene expression in bacteria.

## 6 Cooperativity in Binding: The Case Study of Hemoglobin

So far, our treatment of binding has focused on simple binding reactions such as the myoglobin binding curve in fig. 8 which do not exhibit the sharpness seen in some biological examples. This sharpness in binding is often denoted as “cooperativity” and refers to the fact that in cases where several ligands bind simultaneously, the energy of binding is not additive. In particular, cooperativity refers to the fact that the binding energy for a given ligand depends upon the number of ligands that are already bound to the receptor. Intuitively, the cooperativity idea results from the fact that when a ligand binds to a protein, it will induce some conformational change. As a result, when the next ligand binds, it finds an altered protein interface and hence experiences a different binding energy (characterized by a different equilibrium constant) [33, 34, 12, 13]. From the point of view of statistical mechanics, we will interpret cooperativity as an interaction energy - that is, the energy of the various ligand binding reaction are not simply additive.

The classic example of this phenomenon is hemoglobin, the molecule responsible for carrying oxygen in the blood. This molecule has four distinct binding sites, reflecting its structure as a tetramer of four separate myoglobin-like polypeptide chains [22]. Our treatment of ligand-receptor binding in the case of hemoglobin can be couched in the language of two-state occupation variables. In particular, for hemoglobin, we describe the state of the system with the four variables  $(\sigma_1, \sigma_2, \sigma_3, \sigma_4)$ , where  $\sigma_i$  adopts the values 0 (unbound) or 1 (bound) characterizing the occupancy of site  $i$  within the molecule. One of the main goals of a model like this is to address questions such as the average number of bound oxygen molecules as a function of the oxygen concentration (or partial pressure).

As a first foray into the problem of cooperative binding, we examine a toy model which reflects some of the full complexity of binding in hemoglobin. In particular, we imagine a fictitious dimoglobin molecule which has only two myoglobin-like polypeptide chains and therefore two  $O_2$  binding sites. We begin by identifying the states and weights as shown in fig. 13. This molecule is characterized by four distinct states corresponding to each of the binding sites of the dimoglobin molecule either being occupied or empty. For example, if binding site 1 is occupied we have  $\sigma_1 = 1$  and if unoccupied then  $\sigma_1 = 0$ . The energy of the

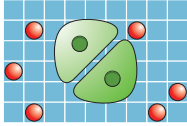
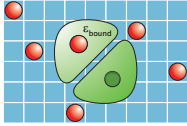
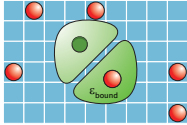
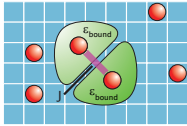
STATE	ENERGY	MULTIPLICITY	WEIGHT (MULTIPLICITY × BOLTZMANN WEIGHT)
	$L\epsilon_{\text{solution}}$	$\frac{\Omega!}{L!(\Omega-L)!} \approx \frac{\Omega^L}{L!}$	$\frac{\Omega^L}{L!} e^{-\beta L\epsilon_{\text{solution}}}$
	$(L-1)\epsilon_{\text{solution}} + \epsilon_{\text{bound}}$	$\frac{\Omega!}{(L-1)!(\Omega-L+1)!} \approx \frac{\Omega^{L-1}}{(L-1)!}$	$\frac{\Omega^{L-1}}{(L-1)!} e^{-\beta[(L-1)\epsilon_{\text{solution}} + \epsilon_{\text{bound}}]}$
	$(L-1)\epsilon_{\text{solution}} + \epsilon_{\text{bound}}$	$\frac{\Omega!}{(L-1)!(\Omega-L+1)!} \approx \frac{\Omega^{L-1}}{(L-1)!}$	$\frac{\Omega^{L-1}}{(L-1)!} e^{-\beta[(L-1)\epsilon_{\text{solution}} + \epsilon_{\text{bound}}]}$
	$(L-2)\epsilon_{\text{solution}} + 2\epsilon_{\text{bound}} + J$	$\frac{\Omega!}{(L-2)!(\Omega-L+2)!} \approx \frac{\Omega^{L-2}}{(L-2)!}$	$\frac{\Omega^{L-2}}{(L-2)!} e^{-\beta[(L-2)\epsilon_{\text{solution}} + 2\epsilon_{\text{bound}} + J]}$

Figure 13: States and weights for dimoglobin. The different states correspond to different occupancies of the two binding sites by oxygen molecules. Cooperativity is captured in this model via an additional energy  $J$  that is present in the case when both sites are occupied. The combinatorial factors in the statistical weights arise from the degrees of freedom associated with the solution in precisely the same way as illustrated in the earlier applications.

system can be written as

$$E = \Delta\epsilon(\sigma_1 + \sigma_2) + J\sigma_1\sigma_2, \quad (37)$$

where  $\Delta\epsilon$  is the energy gain garnered by the molecules when bound to dimoglobin as opposed to wandering around in solution. The parameter  $J$  is a measure of the cooperativity and implies that when both sites are occupied, the energy is more than the sum of the individual binding energies [33, 13].

As we have done throughout the article, we can compute the probability of different states using the states and weights diagram by constructing a ratio with the numerator given by the weight of the state of interest and the denominator by the sum over all states. In analogy to eq. 13 we can write the partition function corresponding to the weights in fig. 13. Next we can calculate the probability of finding no oxygen molecule bound to our dimoglobin molecule, the probability of finding one oxygen molecule bound or that of

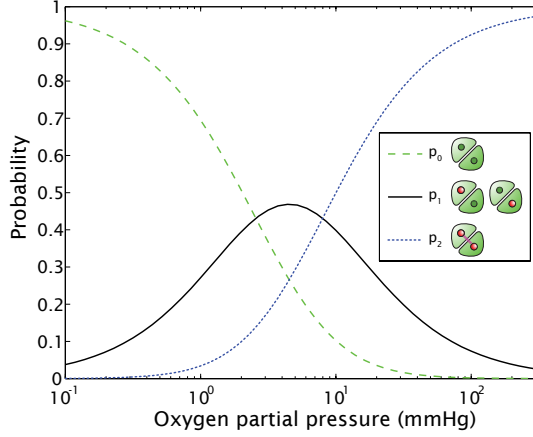


Figure 14: Probabilities of oxygen binding to dimoglobin. The plot shows the probability of finding no oxygen molecules bound to dimoglobin ( $p_0$ ), of finding one molecule bound ( $p_1$ ) and that of finding two molecules bound ( $p_2$ ). The parameters used are  $\Delta\epsilon = -5 k_B T$ ,  $J = -.25 k_B T$ , and  $c_0 = 760$  mmHg.

finding two molecules bound. For example, if we want to compute the probability of single occupancy we can add up the weights corresponding to this outcome of fig. 13 and divide them by the total partition function which yields

$$p_1 = \frac{2 \frac{\Omega^{L-1}}{(L-1)!} e^{-\beta[(L-1)\epsilon_{\text{solution}} + \epsilon_{\text{bound}}]}}{\frac{\Omega^L}{L!} e^{-\beta L \epsilon_{\text{solution}}} + 2 \frac{\Omega^{L-1}}{(L-1)!} e^{-\beta[(L-1)\epsilon_{\text{solution}} + \epsilon_{\text{bound}}]} + \frac{\Omega^{L-2}}{(L-2)!} e^{-\beta[(L-2)\epsilon_{\text{solution}} + 2\epsilon_{\text{bound}} + J]}}. \quad (38)$$

Similarly to what was done in eq. 19 we can write the previous probability in terms of the standard state and multiply and divide by  $\frac{\Omega^L}{L!} e^{-\beta L \epsilon_{\text{solution}}}$ . This results in

$$p_1 = \frac{2 \frac{c}{c_0} e^{-\beta \Delta\epsilon}}{1 + 2 \frac{c}{c_0} e^{-\beta \Delta\epsilon} + \left(\frac{c}{c_0}\right)^2 e^{-\beta \Delta\epsilon + J}}. \quad (39)$$

In fig. 14 we plot this probability as a function of the oxygen partial pressure as well as  $p_0$  and  $p_2$ , the probabilities of the dimoglobin molecule being empty and being occupied by two oxygen molecules, respectively.

Next, we calculate the average number of bound oxygen molecules as a function of its partial pressure. We add the number of molecules bound in each state times the probability

of that state occurring

$$\langle N_{\text{bound}} \rangle = 1 \times p_1 + 2 \times p_2 = \frac{2 \frac{c}{c_0} e^{-\beta \Delta \epsilon} + 2 \left(\frac{c}{c_0}\right)^2 e^{-\beta(2\Delta \epsilon + J)}}{1 + 2 \frac{c}{c_0} e^{-\beta \Delta \epsilon} + \left(\frac{c}{c_0}\right)^2 e^{-\beta(2\Delta \epsilon + J)}}. \quad (40)$$

To further probe the nature of cooperativity, a useful exercise is to examine the occupancy of the dimoglobin molecule in the case where the interaction term  $J$  is zero. We find that the average occupancy is given by the sum of two independent single-site occupancies as

$$\langle N \rangle = \frac{2 \frac{c}{c_0} e^{-\beta \Delta \epsilon} + 2 \left(\frac{c}{c_0}\right)^2 e^{-\beta 2 \Delta \epsilon}}{1 + 2 \frac{c}{c_0} e^{-\beta \Delta \epsilon} + \left(\frac{c}{c_0}\right)^2 e^{-\beta 2 \Delta \epsilon}} = \frac{2 \frac{c}{c_0} e^{-\beta \Delta \epsilon} \left(1 + \frac{c}{c_0} e^{-\beta \Delta \epsilon}\right)}{\left(1 + \frac{c}{c_0} e^{-\beta \Delta \epsilon}\right)^2} = 2 \frac{\frac{c}{c_0} e^{-\beta \Delta \epsilon}}{1 + \frac{c}{c_0} e^{-\beta \Delta \epsilon}}. \quad (41)$$

In considering the real hemoglobin molecule rather than the fictitious dimoglobin, the only novelty incurred is extra mathematical baggage. In this case, there are four state variables  $\sigma_1, \sigma_2, \sigma_3$  and  $\sigma_4$  that correspond to the state of oxygen occupancy at the four distinct sites on the hemoglobin molecule. There are various models that have been set forth for thinking about binding in hemoglobin, many of which can be couched simply in the language of these occupation variables. One important model which was introduced by Adair in 1925 [35] assigns distinct interaction energies for the binding of the second, third and fourth oxygen molecules. The energy in this model is written as

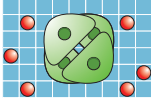
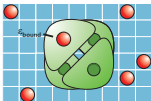
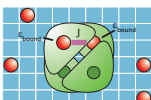
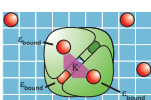
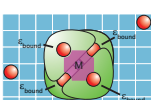
$$E = \Delta \epsilon \sum_{\alpha=1}^4 \sigma_{\alpha} + J \sum_{(\alpha \neq \gamma)=1}^4 \sigma_{\alpha} \sigma_{\gamma} + K \sum_{(\alpha \neq \beta \neq \gamma)=1}^4 \sigma_{\alpha} \sigma_{\beta} \sigma_{\gamma} + M \sum_{(\alpha \neq \beta \neq \gamma \neq \delta)=1}^4 \sigma_{\alpha} \sigma_{\beta} \sigma_{\gamma} \sigma_{\delta}, \quad (42)$$

where the parameters  $K$  and  $M$  capture the energy of the three- and four-body interactions, respectively. This model results in a very sharp response compared to a simple binding curve without any cooperativity [36]. In fig. 15 we show the corresponding states for this model as well as the fit to the experimental data. This curve should be contrasted with the fit curve using the simple binding model such as eq. 19.

## 7 Conclusions

We have argued that statistical mechanics needs to be part of the standard toolkit of biologists who wish to understand the biochemical underpinnings of their discipline. Indeed,

a)

STATE	ENERGY	MULTIPLICITY	WEIGHT (MULTIPLICITY x BOLTZMANN WEIGHT)
	$L\epsilon_{\text{solution}}$	$\frac{\Omega!}{L!(\Omega-L)!} \approx \frac{\Omega^L}{L!}$	$\frac{\Omega^L}{L!} e^{-\beta L\epsilon_{\text{solution}}}$
	$(L-1)\epsilon_{\text{solution}} + \epsilon_{\text{bound}}$	$4 \frac{\Omega!}{(L-1)(\Omega-L+1)!} \approx 4 \frac{\Omega^{L-1}}{(L-1)!}$	$4 \frac{\Omega^{L-1}}{(L-1)!} e^{-\beta[(L-1)\epsilon_{\text{solution}} + \epsilon_{\text{bound}}]}$
	$(L-2)\epsilon_{\text{solution}} + 2\epsilon_{\text{bound}} + J$	$6 \frac{\Omega!}{(L-2)(\Omega-L+2)!} \approx 6 \frac{\Omega^{L-2}}{(L-2)!}$	$6 \frac{\Omega^{L-2}}{(L-2)!} e^{-\beta[(L-2)\epsilon_{\text{solution}} + 2\epsilon_{\text{bound}} + J]}$
	$(L-3)\epsilon_{\text{solution}} + 3\epsilon_{\text{bound}} + 3J + K$	$4 \frac{\Omega!}{(L-3)(\Omega-L+3)!} \approx 4 \frac{\Omega^{L-3}}{(L-3)!}$	$4 \frac{\Omega^{L-3}}{(L-3)!} e^{-\beta[(L-3)\epsilon_{\text{solution}} + 3\epsilon_{\text{bound}} + 3J + K]}$
	$(L-4)\epsilon_{\text{solution}} + 4\epsilon_{\text{bound}} + 6J + 4K + M$	$\frac{\Omega!}{(L-4)(\Omega-L+4)!} \approx \frac{\Omega^{L-4}}{(L-4)!}$	$\frac{\Omega^{L-4}}{(L-4)!} e^{-\beta[(L-4)\epsilon_{\text{solution}} + 4\epsilon_{\text{bound}} + 6J + 4K + M]}$

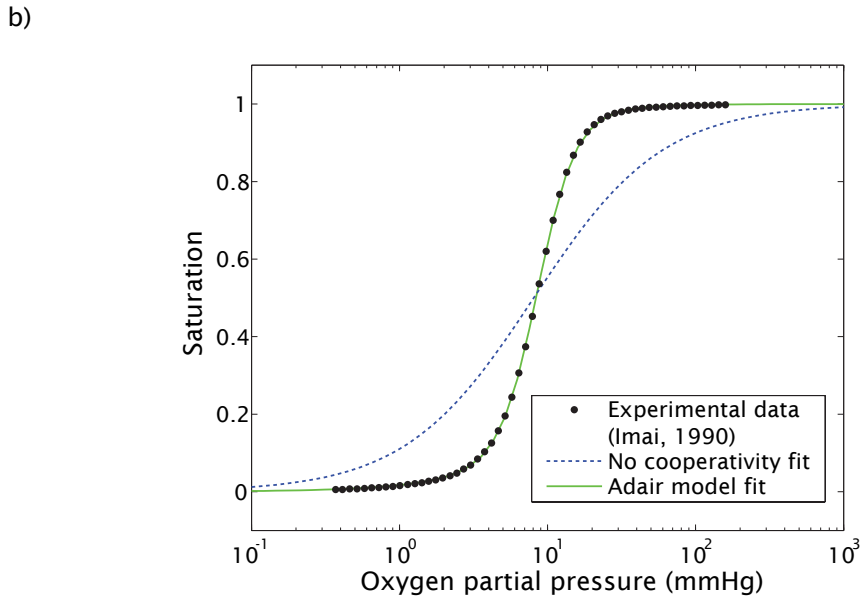


Figure 15: Binding of oxygen by hemoglobin. (a) States and weights for hemoglobin binding in the Adair model. The energy for each state includes the energy of the oxygen molecules left in solution and the energy of bound oxygen. (b) Plot of experimental data [37] together with the data fit to the four parameters of the Adair model and to a simple no-cooperativity case. Note that the shape of the curve without cooperativity looks different from that in fig. 8 only because we plot it here using a log-scale.

the ideas in this paper represent a small part of a more general text on physical biology entitled “Physical Biology of the Cell” worked on by all of us which aims not only to provide the quantitative underpinnings offered by statistical mechanics, but a range of other tools that are useful for the quantitative analysis of living matter. Our own experiments in teaching such material convince us that a first exposure to statistical mechanics can be built around a careful introduction of the concept of a microstate and the assertion of the Boltzmann distribution as the fundamental “law” of statistical mechanics. These formal ideas in conjunction with simple, approximate models such as the lattice model of solution and two-state models for molecular conformations permit an analysis of a large number of different interesting problems.

We challenge the notion that biologists need to understand every detail of statistical mechanics in order to use it fruitfully in their thinking and research. The importance of this dictum was stated eloquently by Schawlow who noted “To do successful research, you don’t need to know everything. You just need to know of one thing that isn’t known.” To successfully apply statistical mechanics, we argue that a feeling for microstates and how to assign them probabilities will go a long way toward demystifying statistical mechanics and permit biology students to think about many new problems.

With the foundations described in this paper in hand, our courses turn to a variety of other interesting applications of statistical mechanics that include: accessibility of nucleosomal DNA, force-extension curves for DNA, lattice models of protein folding, the origins of the Hill coefficient, the role of tethering effects in biochemistry (what we like to call “biochemistry on a leash”), the Poisson-Boltzmann equation, the analysis of polymerization and molecular motors and many more. Though it is easy to make blanket statements about living systems being far from equilibrium, the calculus of equilibrium as embodied in statistical mechanics still turns out to be an exceedingly useful tool for the study of living systems and the molecules that make them work.

## **Appendix: A derivation of the Boltzman distribution**

The setup we consider for our derivation of the probability of microstates for systems in contact with a thermal reservoir is shown in fig. 16 [38, 39]. The idea is that we have a box

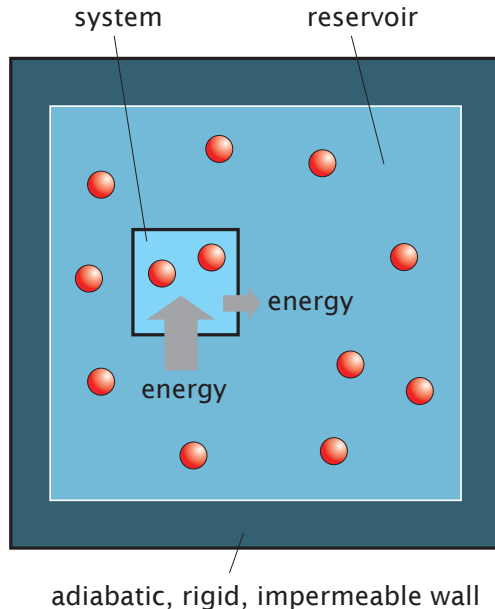


Figure 16: System in contact with a heat bath (thermal reservoir). The system and its reservoir are completely isolated from the rest of the world by walls that are adiabatic (forbid the flow of heat out or in), rigid and impermeable (forbid the flow of matter). Energy can flow across the wall separating the system from the reservoir and as a result, the energy of the system (and reservoir) fluctuate.

which is separated from the rest of the world by rigid, impermeable and adiabatic walls. As a result, the total energy and the total number of particles within the box are constant. Inside this box, we now consider two regions, one that is our *system* of interest and the other of which is the reservoir. We are interested in how the system and the reservoir share their energy.

The total energy is  $E_{tot} = E_r + E_s$  where the subscripts  $r$  and  $s$  signify reservoir and system, respectively. Our fundamental assertion is that the probability of finding a given state of the system  $E_s$  is proportional to the number of states available to the *reservoir* when the system is in this state. That is

$$\frac{p_s^{(1)}}{p_s^{(2)}} = \frac{W_r(E_{tot} - E_s^{(1)})}{W_r(E_{tot} - E_s^{(2)})}, \quad (43)$$

where  $W_r(E_{tot} - E_s^{(1)})$  is the number of states available to the *reservoir*, when the system

is in the particular state  $E_s^{(1)}$ . By constructing the ratio of the probabilities, we avoid ever having to compute the absolute number of states available to the system. The logic is that we assert that the system is in *one* particular microstate that is characterized by its energy  $E_s$ . When the system is assigned this energy, the reservoir has available a particular number of states  $W_r(E_{tot} - E_s)$  which depends upon how much energy,  $E_{tot} - E_s$ , it has. Though the equations may seem cumbersome, in fact, it is the underlying conceptual idea that is the subtle (and beautiful) part of the argument. The point is that the total number of states available to the universe of system plus reservoir when the system is in the particular state  $E_s^{(1)}$  is given by

$$W_{tot}(E_{tot} - E_s^{(1)}) = \underbrace{1}_{\text{states of system}} \times \underbrace{W_r(E_{tot} - E_s^{(1)})}_{\text{states of reservoir}} \quad (44)$$

because we have asserted that the system itself is in one particular microstate which has energy  $E_s^{(1)}$ . Though there may be other microstates with the same energy, we have selected one particular microstate of that energy and ask for its probability.

We now ask what the relative probability between two states is. Basically, instead of counting the number of microstates available to a particular states we calculate the relative difference in microstates available to two given states (1) and (2). This will allow us to calculate the probabilities of each macrostate up to a multiplicative factor. As we saw in the text, this multiplicative factor will be given by the partition function  $Z$ . We can then rewrite eq. 43 as

$$\frac{W_r(E_{tot} - E_s^{(1)})}{W_r(E_{tot} - E_s^{(2)})} = \frac{e^{S_r(E_{tot} - E_s^{(1)})/k_B}}{e^{S_r(E_{tot} - E_s^{(2)})/k_B}}, \quad (45)$$

where we have invoked the familiar Boltzmann equation for the entropy, namely  $S = k_B \ln W$  which can be rewritten as  $W = e^{S/k_B}$ . To complete the derivation, we now note that  $E_s \ll E_{tot}$ . As a result, we can expand the entropy as

$$S_r(E_{tot} - E_s) \approx S_r(E_{tot}) - \frac{\partial S_r}{\partial E}(E_{tot} - E_s), \quad (46)$$

where we have only kept terms that are first order in the differences. Finally, if we recall

the thermodynamic identity  $(\partial S/\partial E) = 1/T$ , we can write our result as

$$\frac{p_s^{(1)}}{p_s^{(2)}} = \frac{e^{-E_s^{(1)}/k_B T}}{e^{-E_s^{(2)}/k_B T}} \quad (47)$$

The resulting probability for finding the system in state  $i$  with energy  $E_s^{(i)}$  is

$$p_s^{(i)} = \frac{e^{-\beta E_s^{(i)}}}{Z}, \quad (48)$$

precisely the Boltzmann distribution introduced earlier.

## Acknowledgments

We are extremely grateful to a number of people who have given us both guidance and amusement in thinking about these problems (and some for commenting on the manuscript): Boo Shan Tseng, Phil Nelson, Dan Herschlag, Ken Dill, Kings Ghosh, Mandar Inamdar. JK acknowledges the support of NSF DMR-0403997 and is a Cottrell Scholar of Research Corporation. RP acknowledges the support of the NSF and the NIH Director's Pioneer Award. HG is grateful for support from both the NSF funded NIRT and the NIH Director's Pioneer Award. JT is supported by the NIH.

## References

- [1] National Research Council (U.S.). Committee on Undergraduate Biology Education to Prepare Research Scientists for the 21st Century. Bio 2010 : transforming undergraduate education for future research biologists, 2003.
- [2] W. Bialek and D. Botstein. Introductory science and mathematics education for 21st-century biologists. *Science*, 303(5659):788–90, 2004.
- [3] N. Wingreen and D. Botstein. Back to the future: education for systems-level biologists. *Nat Rev Mol Cell Biol*, 7(11):829–32, 2006.
- [4] C. J. Lumsden, L. E. H. Trainor, and M. Silverman. Physical theory in biology - interdisciplinary course. *American Journal of Physics*, 47(4):302–308, 1979.

- [5] B. Hoop. Resource letter pppp-1 - physical principles of physiological phenomena. *American Journal of Physics*, 55(3):204–210, 1987.
- [6] S. A. Kane. An undergraduate biophysics program: Curricular examples and lessons from a liberal arts context. *American Journal of Physics*, 70(6):581–586, 2002.
- [7] James P. Keener and James Sneyd. *Mathematical physiology*. Interdisciplinary applied mathematics. Springer, New York, 1998.
- [8] Daniel Charles Mattis. *Statistical mechanics made simple : a guide for students and researchers*. World Scientific, River Edge, NJ, 2003.
- [9] Richard Phillips Feynman, Robert B. Leighton, and Matthew L. Sands. *The Feynman lectures on physics. Volume 3*. Addison-Wesley Pub. Co., Reading, Mass., 1963.
- [10] B. Maier and J. O. Radler. Conformation and self-diffusion of single DNA molecules confined to two dimensions. *Physical Review Letters*, 82(9):1911–1914, 1999.
- [11] Gregorio Weber. *Protein interactions*. Chapman and Hall, New York, 1992.
- [12] Irving M. Klotz. *Ligand-receptor energetics : a guide for the perplexed*. John Wiley & Sons, New York, 1997.
- [13] Ken A. Dill and Sarina Bromberg. *Molecular driving forces : statistical thermodynamics in chemistry and biology*. Garland Science, New York, 2003. This book illustrates a diverse array of uses of lattice models to examine interesting problems in statistical physics.
- [14] A. P. Minton. The influence of macromolecular crowding and macromolecular confinement on biochemical reactions in physiological media. *J Biol Chem*, 276(14):10577–80, 2001.
- [15] C. Grosman, M. Zhou, and A. Auerbach. Mapping the conformational wave of acetylcholine receptor channel gating. *Nature*, 403(6771):773–6, 2000.
- [16] G. A. Woolley and T. Loughheed. Modeling ion channel regulation. *Curr Opin Chem Biol*, 7(6):710–4, 2003.

- [17] B. U. Keller, R. P. Hartshorne, J. A. Talvenheimo, W. A. Catterall, and M. Montal. Sodium channels in planar lipid bilayers. channel gating kinetics of purified sodium channels modified by batrachotoxin. *J Gen Physiol*, 88(1):1–23, 1986.
- [18] L. N. Johnson and R. J. Lewis. Structural basis for control by phosphorylation. *Chem Rev*, 101(8):2209–42, 2001.
- [19] Christopher Walsh. *Posttranslational modification of proteins : expanding nature's inventory*. Roberts and Co. Publishers, Englewood, Colo., 2006.
- [20] W. Zhong, J. P. Gallivan, Y. Zhang, L. Li, H. A. Lester, and D. A. Dougherty. From *ab initio* quantum mechanics to molecular neurobiology: a cation-pi binding site in the nicotinic receptor. *Proc Natl Acad Sci U S A*, 95(21):12088–93, 1998.
- [21] L. Bintu, N. E. Buchler, H. G. Garcia, U. Gerland, T. Hwa, J. Kondev, and R. Phillips. Transcriptional regulation by the numbers: models. *Curr Opin Genet Dev*, 15(2):116–24, 2005.
- [22] Eraldo Antonini and Maurizio Brunori. *Hemoglobin and myoglobin in their reactions with ligands*. North-Holland Pub. Co., Amsterdam,, 1971.
- [23] Charles Janeway. *Immunobiology : the immune system in health and disease*. Garland Science, New York, 6th edition, 2005.
- [24] A. Rossi-Fanelli and E. Antonini. Studies on the oxygen and carbon monoxide equilibria of human myoglobin. *Arch Biochem Biophys*, 77(2):478–92, 1958.
- [25] D. W. Brighty, M. Rosenberg, I. S. Chen, and M. Ivey-Hoyle. Envelope proteins from clinical isolates of human immunodeficiency virus type 1 that are refractory to neutralization by soluble cd4 possess high affinity for the cd4 receptor. *Proc Natl Acad Sci U S A*, 88(17):7802–5, 1991.
- [26] V. Weiss, F. Claverie-Martin, and B. Magasanik. Phosphorylation of nitrogen regulator i of escherichia coli induces strong cooperative binding to dna essential for activation of transcription. *Proc Natl Acad Sci U S A*, 89(11):5088–92, 1992.
- [27] G. K. Ackers, A. D. Johnson, and M. A. Shea. Quantitative model for gene regulation by lambda phage repressor. *Proc Natl Acad Sci U S A*, 79(4):1129–33, 1982.

- [28] N. E. Buchler, U. Gerland, and T. Hwa. On schemes of combinatorial transcription logic. *Proc Natl Acad Sci U S A*, 100(9):5136–41, 2003.
- [29] L. Bintu, N. E. Buchler, H. G. Garcia, U. Gerland, T. Hwa, J. Kondev, T. Kuhlman, and R. Phillips. Transcriptional regulation by the numbers: applications. *Curr Opin Genet Dev*, 15(2):125–35, 2005.
- [30] M. Jishage and A. Ishihama. Regulation of RNA polymerase sigma subunit synthesis in *escherichia coli*: intracellular levels of sigma 70 and sigma 38. *J Bacteriol*, 177(23):6832–5, 1995.
- [31] U. Gerland, J. D. Moroz, and T. Hwa. Physical constraints and functional characteristics of transcription factor-DNA interaction. *Proc Natl Acad Sci U S A*, 99(19):12015–20, 2002.
- [32] S. Oehler, M. Amouyal, P. Kolkhof, B. von Wilcken-Bergmann, and B. Müller-Hill. Quality and position of the three *lac* operators of *E. coli* define efficiency of repression. *Embo J*, 13(14):3348–55, 1994.
- [33] Terrell L. Hill. *Cooperativity theory in biochemistry : steady-state and equilibrium systems*. Springer-Verlag, New York, 1985.
- [34] G. K. Ackers and F. R. Smith. Effects of site-specific amino acid modification on protein interactions and biological function. *Annu Rev Biochem*, 54:597–629, 1985.
- [35] G. S. Adair. The hemoglobin system. VI. The oxygen dissociation curve of hemoglobin. *Journal of Biological Chemistry*, 63:529 – 545, 1925.
- [36] L. Pauling. The oxygen equilibrium of hemoglobin and its structural interpretation. *Proc Natl Acad Sci U S A*, 21(4):186–91, 1935.
- [37] K. Imai. Precision determination and Adair scheme analysis of oxygen equilibrium curves of concentrated hemoglobin solution. A strict examination of Adair constant evaluation methods. *Biophys Chem*, 37(1-3):197–210, 1990.
- [38] Charles Kittel and Herbert Kroemer. *Thermal physics*. W.H. Freeman, New York, 2nd edition, 1980.

- [39] F. Reif. *Fundamentals of statistical and thermal physics*. McGraw-Hill, New York,, 1965.